TÜBİTAK

Turkish Journal of Chemistry

http://journals.tubitak.gov.tr/chem/

Research Article

Turk J Chem
(2019) 43: 926 – 935
© TÜBİTAK
doi:10.3906/kim-1807-132

Parameterization, kinetics, and adsorption isotherm of electrocoagulation process of bromothymol blue in aqueous medium using aluminum electrodes

Okon ABAKEDI, Victor MKPENIE*, John OKAFOR
Laboratory of Physical and Inorganic Chemistry, Department of Chemistry, University of Uyo, Uyo, Nigeria

Received: 29.07.2018 • **Accepted/Published Online:** 27.03.2019 • **Final Version:** 11.06.2019

Abstract: The removal of bromothymol blue (BTB) from aqueous solution was studied by electrocoagulation (EC) technique using aluminum electrodes. The various experimental conditions known to influence the EC process were parameterized, including the effects of temperature, concentration, current density, pH, and treatment time. The results obtained have shown that optimum removal efficiency of 99.9% was realized at a current density of 20 mA/cm^2 and pH of 4.7. The adsorption process showed a pseudo-first-order kinetic model as the best fit to the EC data. Freundlich and Langmuir adsorption isotherms supported the adsorption of BTB on aluminum hydroxide being the in situ generated electrocoagulant. From the thermodynamic parameters, the adsorption of BTB is spontaneous, as indicated by the negative value of the Gibbs free energy.

Key words: Electrocoagulation, bromothymol blue, aluminum electrodes, kinetic models, Langmuir isotherm, Freundlich isotherm

1. Introduction

Water is a vital component of life. It is important not only for nature, but also for humans. It plays a significant role in agriculture for growing crops and in industries for production of valuable goods and materials. It is the life-sustaining factor in marine ecosystems. Human populations cannot survive without water as it is used for drinking. The rapid growth of industries and other developmental agencies in recent times has led to the pollution of the water system, leading to environmental issues. The need for clean and potable water systems has been on an upward trend. A constant effort to protect water resources is being made by various governments through the introduction of increasingly strict legislation covering pollutant release.[1]

The textile industry is one of the water-intensive consumers in the world that release large amounts of wastewater into the environment. The effluent contains considerable quantities of various chemicals and dyes.[2] Discharged wastewater containing dyestuff prevents light penetration into aqueous media such as lakes and rivers. It reduces the amount of dissolved oxygen and increases chemical oxygen demand, thereby disrupting aquatic life. In addition, dye colors persist in the environment for longer periods due to high thermal and optimal stability.[3] The presence of colored contaminants even at levels of less than 1 mg L^{-1} is visible and unfavorable in terms of physical properties,[4] creating a need for efficient treatment techniques and methods.

In recent years, the electrocoagulation (EC) process has been investigated and proven as an efficient method for the treatment of dye-contaminated and textile wastewater,[5–7] removal of metal ions from

*Correspondence: vicmkpenie1@gmail.com

wastewater,[8] remediation of pulp and paper industry wastewater,[9] separation of oil from wastewater,[10] treatment of palm oil mill effluent,[11] treatment of nitrate-contaminated water,[12] and removal of phosphate from river water.[13] Some organic compounds removed by the EC process include herbicides,[14] cephalosporin-based antibiotics,[15] and humic acid.[16] EC is an electrochemical approach, which uses an electrical current to remove metals from solutions and is effective in removing suspended solids, dissolved metals, tannins, and dyes. The electrical current provides electromotive force to drive the chemical reactions forcing the elements or compounds to approach the most stable state.[17] The major steps involved in the EC process include electrolytic reactions at electrode surfaces, generation of coagulant in situ by dissolving the electrode electrically, and adsorption of pollutants on coagulants.[18,19] With aluminum electrodes, the following reactions occur at the electrodes:[20]

$$\text{Anode reaction: } Al_{(s)} \rightarrow Al^{3+}_{(aq)} + 3e- \tag{1}$$

$$\text{Cathode reaction: } 2H_2O_{(l)} + 2e^- \rightarrow H_{2(g)} + 2OH^-_{(aq)} \tag{2}$$

At the anode, metal ion is generated (Eq. (1)), and hydrogen gas is released at the cathode (Eq. (2)). The Al^{3+} and OH^- ions generated during the electrochemical process react to form various monomeric and polymeric species and transform into $Al(OH)_3$.[21] The $Al(OH)_3$ flocs capture the dye molecules present in the solution by precipitation and adsorption. The hydrogen gas also helps to remove the flocculated particles from the water.[22]

In our previous work on EC, we investigated azo-2-naphthol,[23] a compound widely used as a dye in industries. In the present study, we investigate the EC of bromothymol blue (BTB) (**1**), which acts as a weak acid in solution. The protonated, deprotonated, or neutral form appears yellow, blue, or green, respectively, in solution. There is no reported work on the EC of BTB in the literature. To the best of our knowledge, this is the first time such a study is undertaken. It is interesting to see that the EC data obtained from this study have been used to determine the adsorption isotherm that is obeyed by the process. The kinetic parameters of the EC process have also been investigated and the optimum conditions for effective removal of BTB from an aqueous medium have been parameterized.

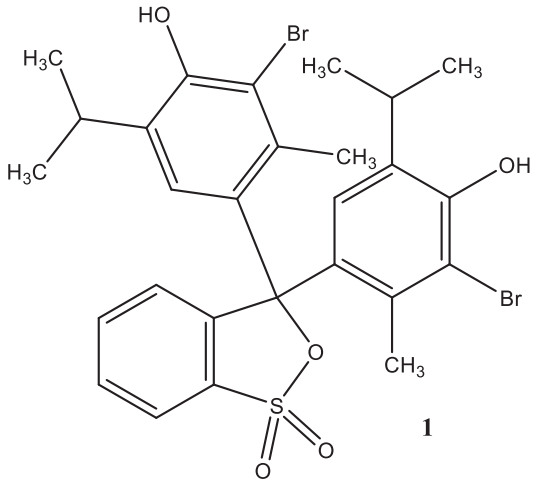

1

1: 3,3-Bis(3-bromo-4-hydroxy-5-isopropyl-2-methyphenyl)-3*H*-benzo[c][1,2]oxathiole 1,1-dioxide

2. Results and discussion

2.1. Effect of the initial pH

EC was first evaluated at different pH levels to determine the optimum pH needed for removal of BTB in aqueous solution. By varying the pH between 2.5 and 8, it became obvious that pH had a significant effect on the color removal efficiency (CRE), as indicated in Figure 1. The optimum pH for the removal of BTB appeared to be 4.7 with efficiency of 78% in the first 15 min and 98% after 45 min of EC time. The optimum pH remained at 4.7 during the different time treatments mapped at 15, 30, and 45 min. This pH value is in agreement with the optimum pH range, 4.5–5.5, reported for aluminum electrodes.[24]

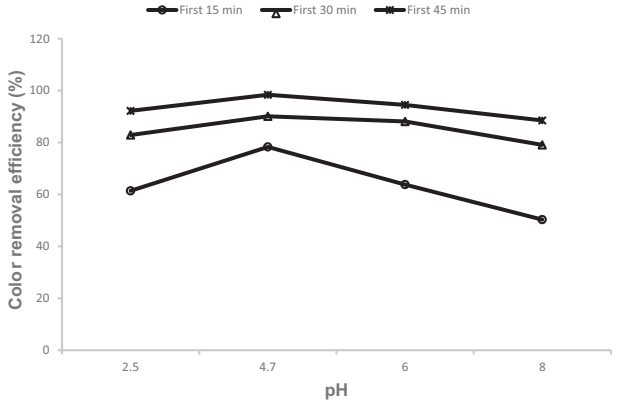

Figure 1. Effect of initial pH on the removal efficiency of bromothymol blue at 20 mA cm^{-2} and 30 °C.

2.2. Effect of the initial dye concentration

Initial dye concentration influences the efficiency of EC processes. The different initial dye concentrations in the range of 20–100 mg L^{-1} were treated at constant current densities and optimum pH for 60 min. The removal efficiency as a function of initial concentration and treatment time are presented in Figures 2 and 3. The results showed that increasing the concentration of BTB from 20 mg L^{-1} to 100 mg L^{-1} led to a decrease in efficiency from 61% to 28% in the first 5 min of EC, 86% to 56% in the first 10 min, and 99.8% to 97.9% after 60 min of EC. This indicates that greater amounts of BTB molecules are removed from the aqueous system at a lower concentration more effectively than at a higher concentration. This may be attributed to some factors in connection with the pathway for BTB removal since adsorption of the molecule on the metallic hydroxide flocs is the major mechanism for the removal. Larger molecular surface of BTB compared to the coagulant, overcrowding on the surface of the coagulant due to limited adsorption sites, and limited amount of coagulant produced being insufficient to service the higher number of BTB molecules may contribute to low adsorption of BTB at higher concentrations. This observation is in agreement with the work of Nasser et al.[25]

2.3. Effect of current density

The data shown in Figures 2 and 3 also reveal the effect of current density on the EC of BTB. The removal efficiency of BTB from aqueous solution increased with an increase in current density. The first 5 min of EC time recorded a CRE of 41.0% for 10 mA cm^{-2} and 47.3% for 20 mA cm^{-2}. At the end of 60 min of EC time, CRE of 98.6% and 99.9% was recorded for 10 mA cm^{-2} and 20 mA cm^{-2}, respectively. Such higher efficiency as a result of the increase in current density may be due to an increase in anode dissolution as the

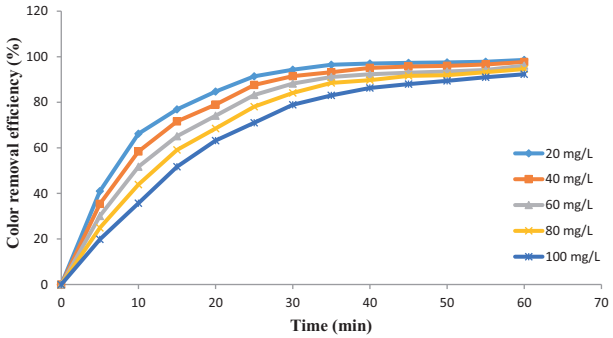

Figure 2. Effect of the initial concentration on CRE of BTB at 10 mA cm^{-2}, 30 °C, and pH 4.7.

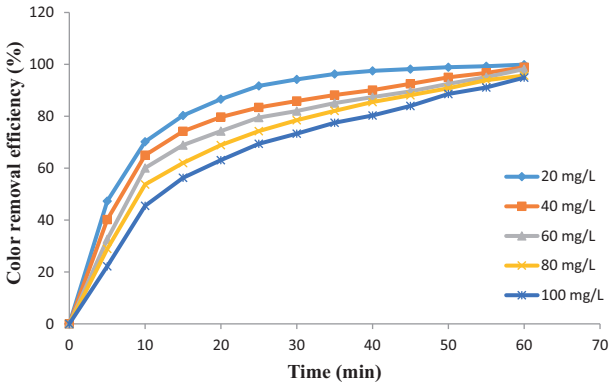

Figure 3. Effect of the initial concentration on CRE of BTB at 20 mA cm^{-2}, 30 °C, and pH 4.7.

current density increases. This leads to an increase in the number of metal hydroxides flocs formed, resulting in increased removal efficiency of BTB.

2.4. Effect of treatment time

The effect of the time of treatment on EC of BTB is presented in Figure 4. EC time is seen to have a significant influence on the CRE. CRE increases as the EC time increases. For the optimum concentration of 20 mg L^{-1}, the CRE rises from 41% in the first 5 min to 98.6% at 60 min of EC time at the current density of 10 mA cm^{-2}, and from 47.3% to 99.9% at the current density of 20 mA cm^{-2}. The EC process of BTB appears to be moderate for all the concentrations studied. The EC point (ECp) for 20 mg L^{-1} BTB solution was reached within 35 min of EC time. The 40 mg L^{-1} solution showed ECp of 37 min while other higher concentrations, namely 60 mg L^{-1}, 80 mg L^{-1}, and 100 mg L^{-1}, had longer ECp of 40 min, 45 min, and 55 min, respectively. Thus, by increasing the concentration of BTB, a longer time period is required to reach the ECp. The results showed that more than 90% CRE was achieved at the ECp at all concentrations ranging from 96.6% (20 mg L^{-1}) to 90.1% (100 mg L^{-1}).

2.5. Effect of temperature

Temperature increase generally leads to an increase in activity since the molecules are able to vibrate at a higher frequency. The EC process in the same manner indicates an increase in EC activity culminating in increased CRE of BTB, as shown in Figure 5. Higher temperature influences the destruction of aluminum oxide film on the anode surface[26] and also increases the rate of adsorption of BTB by the coagulant generated.

2.6. Kinetic studies

The kinetics of the EC of BTB in aqueous solution were studied using three kinetic models. They include a pseudo-first-order kinetic model (Eq. (3)),[27] pseudo-second-order kinetic model (Eq. (4)),[27] and Elovich kinetic model (Eq. (5)).[28]

$$\ln(q_e - q_t) = \ln q_e - k_1 t \tag{3}$$

Here, k_1 is the pseudo-first-order constant (min^{-1}), q_t is the amount of adsorbate per unit mass of adsorbent at contact time t (mg g^{-1}), and q_e is the amount of adsorbate per unit mass of adsorbent at equilibrium (mg

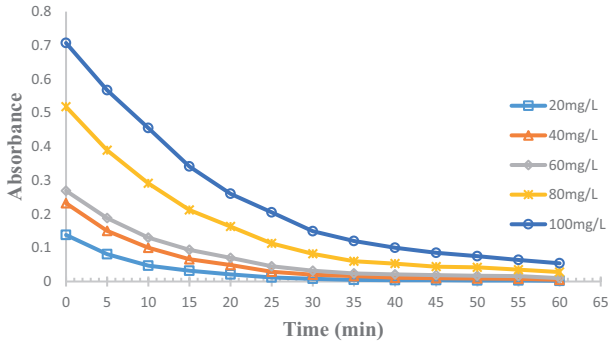

Figure 4. Plots of absorbance vs. electrolysis time for different concentrations of BTB in aqueous solution at 30 °C, 10 mA cm^{-2}, and pH 4.7.

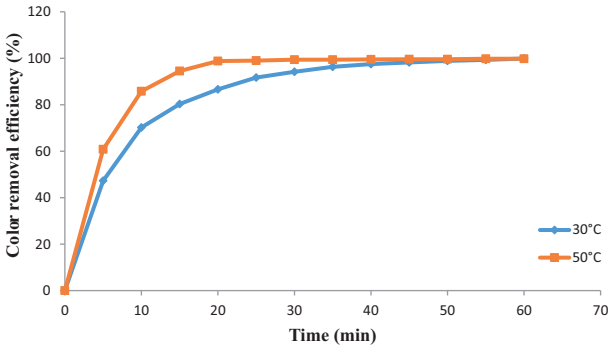

Figure 5. Effect of the temperature on the CRE of BTB at 20 mg L^{-1}, 20 mA cm^{-2}, and pH 4.7.

g^{-1}).

$$\frac{t}{q_t} = \frac{1}{k_2 q_e 2} + \frac{t}{q_e} \tag{4}$$

Here, k_2 is the rate constant of the pseudo-second-order reaction (g mg^{-1} min^{-1}).

$$q_t = \frac{1}{\beta} ln\,(\alpha\beta) + \frac{1}{\beta} \ln t \tag{5}$$

Here, q_t is the sorption capacity at time t (mg g^{-1}), α is the initial sorption rate (mg g^{-1} min^{-1}), and β is the desorption constant (g mg^{-1}).

The kinetic parameters of the EC process of BTB obeyed the pseudo-first-order kinetic model, giving a linear slope with a high correlation coefficient (R^2) for all the concentrations of BTB solutions and temperatures studied (Figures 6 and 7). The EC data gave a nearly linear plot with pseudo-second-order and Elovich kinetic models (see Supplementary information).

The kinetic parameters for the pseudo-first-order model are summarized in Table 1 while those for the pseudo-second-order and Elovich models are presented in the Supplementary information. Higher R^2 values were obtained for the pseudo-first-order kinetic model compared to the pseudo-second-order kinetic model. Hence,

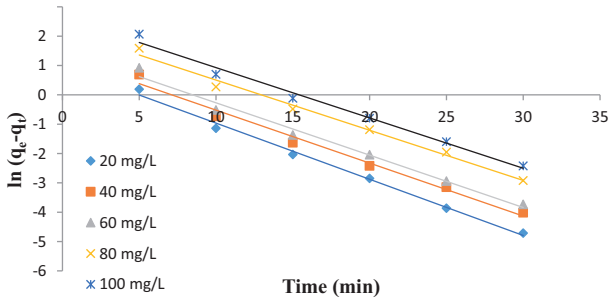

Figure 6. Pseudo-first-order plot of the EC of BTB at 20 mA cm^{-2}, pH 4.7, and 30 °C.

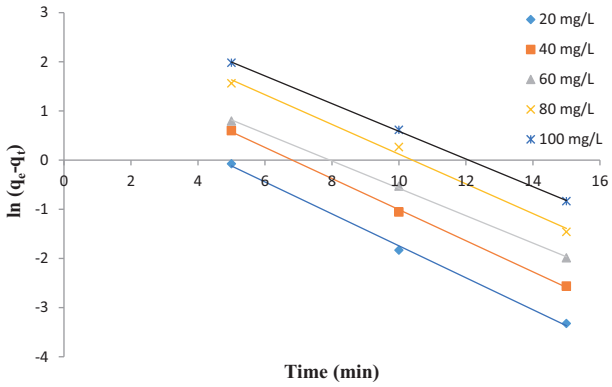

Figure 7. Pseudo-first-order plot of the EC of BTB at 20 mA cm^{-2}, pH 4.7, and 50 °C.

the EC of BTB dye followed the pseudo-first-order kinetic model. Additionally, better correlation coefficients were obtained at 50 °C compared to 30 °C, depicting a better EC process at increased temperature.

Table 1. Pseudo-first-order kinetic parameters for the EC of BTB.

Pseudo-first-order								
	30 °C				50 °C			
Conc.	k_1	q_e (Exp)	q_e (Cal)	R^2	k_1	q_e (Exp)	q_e (Cal)	R^2
(mg/L)	(min^{-1})	(mg g^{-1})	(mg g^{-1})		(min^{-1})	(mg g^{-1})	(mg g^{-1})	
20	0.191	2.588	0.340	0.994	0.281	4.509	0.609	0.997
40	0.180	3.611	0.524	0.985	0.302	8.637	0.998	0.999
60	0.178	4.531	0.585	0.985	0.278	9.107	1.128	0.999
80	0.171	9.143	1.086	0.989	0.316	23.22	2.076	0.993
100	0.171	14.04	1.400	0.986	0.325	30.02	2.702	0.999

2.7. Adsorption isotherms

Several adsorption isotherms were used to investigate the mode of adsorption of BTB on the electrode surface during the EC process and the Freundlich and Langmuir isotherms provided the best fit. The Langmuir adsorption isotherm can be expressed according to Eq. (6).[27]

$$q_e = \left(\frac{q_{\max} K_L C_e}{1 + K_L C_e}\right) \tag{6}$$

Here, q_e is the solid phase adsorbate concentration at equilibrium (mg/g), q_{max} is the maximum adsorption capacity corresponding to complete monolayer coverage on the surface (mg g^{-1}), C_e is the concentration of adsorbate at equilibrium (mg L^{-1}), and K_L is the Langmuir constant (L mg^{-1}).

The dimensionless constant R_L, which is characteristic of the Langmuir adsorption isotherm, is given by Eq. (7).[29]

$$R_L = \frac{1}{1 + K_L C_o} \tag{7}$$

Here, K_L is the Langmuir constant, while C_o is the initial concentration of the BTB in aqueous solution. When the value of R_L lies between 0 and 1, it implies a favorable adsorption. In the present work, the R_L values were found to be between 0 and 1 for the adsorption of BTB. Similar R_L values have been reported in the literature.[14,30]

The Freundlich adsorption isotherm is given by Eq. (8).[27]

$$q_e = K_F C_e^{\frac{1}{n}} \tag{8}$$

Here, K_F is the Freundlich constant that indicates the adsorption capacity of the adsorbent (L gm^{-1}), and n is an empirical constant related to the magnitude of the adsorption driving force.

Eq. (6) can be rearranged to give a linear equation expressed as Eq. (9); a plot of C_e/q_e against C_e yields a straight line with a slope of $1/q_{max}$ and intercept of $1/(q_{max} K_L)$.

$$\frac{\mathbf{C_e}}{\mathbf{q_e}} = \frac{\mathbf{1}}{\mathbf{q_{max} K_L}} + \frac{\mathbf{C_e}}{\mathbf{q_{max}}} \tag{9}$$

Eq. (8) can be rearranged to give a linear equation expressed as Eq. (10); a plot of $\ln q_e$ versus $\ln C_e$ gives a straight line with a slope of 1/n and intercept of $\ln K_F$.

$$\ln q_e = ln\, K_F + \frac{1}{n} ln\, C_e \tag{10}$$

Langmuir and Freundlich adsorption isotherms plots for EC of BTB are shown in the Supplementary information. The data obtained for the adsorption of BTB on the electrode surface could be better explained using the Freundlich isotherm model since it shows higher R^2 values than the Langmuir model (Table 2). The values of Freundlich constant n obtained in this work were 2.409 and 2.084 at 30 °C and 50 °C, respectively (Table 2). Comparatively, an n value of 1.02944 was reported by Kamaraj et al.[14] for the adsorption of an herbicide (2,4-DP) on the $Al(OH)_3$ surface. When the value of n ranges between 1 and 10, favorable adsorption is implied.[14] Hence, BTB was favorably adsorbed on the $Al(OH)_3$ surface.

Table 2. Some parameters of the linear regression of Freundlich and Langmuir isotherms for the EC of BTB in aqueous solution.

			Langmuir isotherm		
Temp.	q_{max}	K_L	R_L	R^2	ΔG
(°C)	(mg g^{-1})	(L mg^{-1})			(kJ mol^{-1})
30	1.779	18.546	0.0027	0.879	–7.357
50	3.086	54.007	0.0092	0.954	–10.712
			Freundlich isotherm		
Temp	n	K_F	R^2	ΔG	
(°C)		(mg g^{-1})		(kJ mol^{-1})	
30	2.409	2.686	0.9315	–2.489	
50	2.084	13.271	0.9936	–4.861	

2.8. Adsorption thermodynamics

The free energy change (ΔG) for the EC process was calculated using the expression in Eq. (11).[29,31]

$$\Delta G = -RT \ln K \tag{11}$$

Here, ΔG is the free energy (kJ/mol), K is the equilibrium constant, R is the gas constant, and T is the absolute temperature.

The values of the thermodynamic parameters K and ΔG are presented in Table 2. The values of K were obtained from the Langmuir and Freundlich isotherm plots (see Supplementary information), respectively. The negative values of ΔG for the EC process indicate spontaneity of the process and the stability of the adsorbed layer on the coagulant surface.

2.9. Conclusions

The optimum parameters necessary for the EC of BTB in aqueous solution have been characterized. These include pH, initial concentration, current densities, treatment time, and temperature. The CRE of BTB has been shown to increase with treatment time, current densities, and temperature while the efficiency decreased

with initial concentration. The EC data support a pH of 4.7 as the optimum pH for the removal of BTB and also fit well into the pseudo-first-order kinetic model. The adsorption of BTB on the aluminum electrode surface has been shown to obey Langmuir and Freundlich adsorption isotherms with negative thermodynamic parameter (ΔG) indicating spontaneity of the EC process.

3. Experimental

3.1. General

Analytical grade reagents were used throughout the work. BTB was obtained from May & Baker (M&B) Limited, UK. Sodium hydroxide was obtained from Kermel, China. Sodium chloride was obtained from BDH Laboratory Supplies, UK. Hydrochloric acid was obtained from Fischer Scientific Limited, UK. Distilled-deionized (D-D) water was used throughout the experiment. The absorbance of the solution was recorded using a UV/Vis spectrophotometer (Jenway 7305). The LWDQGS APR-3002 model DC power supply system was employed to provide the required direct current with maximum current of 2 A.

3.2. Preparation of the BTB solutions for EC

The BTB stock solution was prepared by dissolving 2 g of the BTB in 2 L of D-D water. The resulting stock solution (1 g L^{-1}) was scanned through 200–800 nm wavelengths using a UV-Vis spectrophotometer to obtain the wavelength of maximum absorption. The absorption maximum λ_{max} for the BTB solution was recorded as 440 nm. The stock solution was diluted to give working concentrations of 20 mg L^{-1}, 40 mg L^{-1}, 60 mg L^{-1}, 80 mg L^{-1}, and 100 mg L^{-1}.

3.3. EC setup and procedure

EC was performed in a 500-mL beaker, which acted as the EC tank with 400 mL as the volume of the BTB solution. Two aluminum electrodes (anode and cathode) with dimensions of 4 cm $\times$12 cm were dipped in the tank and were placed 2 cm apart. The aluminum electrodes were immersed 5 cm into the solution with a total area of 40 cm^2. The electrodes were connected to a DC power supply having a maximum current of 2 A. The EC setup was placed on a magnetic stirrer hot plate with a Teflon bar rotating at a velocity of 360 rpm for agitation of the solution throughout the duration of the experiment. The supporting electrolyte used in this experiment was sodium chloride (0.2 g). The two aluminum electrodes were connected to the DC supply. The initial absorbance of the BTB solution was measured by means of the UV-Vis spectrophotometer. At 5-min intervals over a 1-h period of electrolysis, aliquots of the solution (5 mL) were withdrawn and centrifuged, and the absorbance of the supernatant solution was measured at the wavelength corresponding to the absorption maximum (440 nm) for the BTB solution. The EC process was carried out varying the following operational parameters: current densities 10 mA cm^{-2} and 20 mA cm^{-2}; temperatures 30 °C and 50 °C; pH 2.5, 4.7, 6, and 8 for each working concentration of 20, 40, 60, 80, and 100 mg L^{-1}. The pH of the solution was adjusted to the required value with 1 M HCl and 1 M NaOH for the acid and alkaline ranges, respectively. The absorbance data were then used to determine the CRE (%) of the BTB using Eq. (12).[32]

$$CRE(\%) = (\frac{C_o - C_T}{C_o}) \times 100 \tag{12}$$

Here, C_o is the initial absorbance of the BTB solution before the EC process and C_T is the absorbance of the solution at different time intervals during the EC process.

The amount of coagulant generated was estimated with Eq. (13).[33]

$$W = \frac{(I\,x\,t\,x\,M)}{z\,x\,F} \tag{13}$$

Here, W is the amount of electrode dissolved in grams, I is the current intensity in amperes, t is time in seconds, M is the relative molar mass of the electrode, z is number of electrons in the redox reaction, and F is the Faraday constant (96500 C).

References

1. Bazrafshan, E.; Mohammadi, L.; Moghaddan, A. A.; Mahvi, A. H. *J. Environ. Health Sci. Eng.* **2015**, *13*, 1-16.
2. Sun, D.; Zhang, X.; Wu, Y.; Lui, X. *J. Hazard. Mater.* **2010**, *181*, 335-342.
3. Couto, S. R. *Biotechnol. Adv.* **2009**, *27*, 227-235.
4. Ghaneian, M. T.; Ghanzadeh, G.; Gholami, M.; Ghaderinasab, F. *Zahedan. J. Res. Med. Sci.* **2010**, *11*, 25-34.
5. Salmani, E. R.; Ghobanian, A.; Ahmadzadeh, S.; Dolatabadi, M.; Nemanifar, N. *Iranian Journal of Health, Safety, and Environment* **2016**, *3*, 403-417.
6. Khandegar, V.; Saroha, A. K. *J. Environ. Manage.* **2013**, *128*, 949-963.
7. Naje, A. S.; Chelliapan, S.; Zakaria, Z.; Abbas, S. A. *Int. J. Electrochem. Sci.* **2015**, *10*, 4495-4512.
8. Aber, S.; Amani-Ghadim, A. R.; Mirzajani, V. J. *J. Hazard. Mater.* **2009**, *171*, 484-490.
9. Kumar, D.; Gaurav, V. K.; Sharma, C. *American Journal of Plant Sciences* **2018**, *9*, 2462-2479.
10. Fadali, O. A.; Ebraheim, A. A.; El-Gamil, A.; Altaher, H. *J. Environ. Sci. Technol.* **2016**, *9*, 62-74.
11. Sayuti, S. C.; Mohd Azoddein, A. A. *Malaysian J. Anal. Sci.* **2015**, *19*, 663-668.
12. Deghani, M.; Hoseini, M.; Fath-Aabaadi, M. F.; Elhamiyan, Z.; Shamsedini, N.; Ghanbarian, M.; Nourozi, A. *Jundishapur. J. Health. Sci.* **201**6, *8*, 1-11.
13. Hashim, K. S.; Khaddar, R. A.; Jasim, N.; Shaw, A.; Phipps, D.; Kot, P.; Pedrola, M. O.; Alattabi, A. W.; Addulredha, M.; Alwsh, R. *Sep. Purif. Technol.* **2019**, *210*, 135-144.
14. Kamaraj, R.; Davidson, D. J.; Sozhan, G ; Vasudevan, S. *RSC Adv.* **2015**, *5*, 39799-39809.
15. Pandiarajan, A.; Kamaraj, R.; Vasudevan, S. *New J. Chem.* **2017**, *41*, 4518-4530.
16. Alimohammadi, A.; Askari, M.; Dehghami, M. H.; Dalvand, A.; Saeed, R.; Yetilmezsoy, K.; Heibati, B.; McKay, G. *Int. J. Environ. Sci. Technol.* **2017**, *14*, 2125-2134.
17. Mkpenie, V. N.; Essien, E. A.; Etim, U. J. *Int. J. Sci. Res.* **2014**, *3*, 292-295.
18. Daneshvar, N.; Oladegaragoze, A.; Djafarzadeh, N. *J. Hazard. Mater.* **2006**, *129*, 116-122.
19. Holt, P. K.; Barton, G. W.; Mitchell, C. A. *Chemosphere* **2005**, *59*, 355-367.
20. Harif, T.; Khai, M. Adin, A. *Water Res.* **2012**, *46*, 3177-3188.
21. Deb, T. K.; Majumdar, S. *Int. J. Environ. Bioener.* **2013**, *6*, 96-116.
22. Bazrafshan, E.; Ownagh, K. A.; Mahvi, A. H. *E-Journal of Chemistry* **2012**, *9*, 2297-2308.
23. Mkpenie, V. N.; Abakedi, O. U. *Curr. Res. Chem.* **2015**, *7*, 34-43.
24. Mkpenie, V. N.; Udo, U. *AASCIT J. Chem.* **2015**, *2*, 116-122.
25. Nasser, M. G.; Alaa, M. S.; Nader, B. F. *J. Chem. Eng. Process Technol.* **2016**, *7*, 269-275.
26. Chen, G. H. *Sep. Purif. Technol.* **2004**, *38,* 11-41.
27. Malakootain, M.; Moosazadeh, M.; Yousefi, N.; Fatehizadeh, A. *Afr. J. Environ. Sci. Technol.* **2011**, *5*, 299-306.
28. Zohre, S.; Ataallah, S. G.; Mehdi, A. *J. Water Environ. Eng.* **2010**, *2*, 16-28.

29. Vasudevan, S.; Lakshmi, J.; Sozhan, G. *Water Environ. Res.* **2012**, *84*, 209-219.
30. Kamaraj, R.; Pandiarajan, A.; Gandhi, M. R.; Shibayama, A.; Vasudevan, S. *Chem. Select* **2017**, *2*, 342-355.
31. Kamaraj, R.; Pandiarajan, A.; Jayakiruba, S.; Naushad, M.; Vasudevan, S. *J. Mol. Liq.* **2016**, *215*, 204-211.
32. Ghanim, A. N.; Ajjam, S. K. *Civil Environ. Res.* **2013**, *3*, 64-73.
33. Parga, J. R.; Vasquez, V.; Moreno, H. *J. Metall.* **2009**, *2009*, 1-9.

Supplementary information

Table S1. Electrocoagulation results for treatment of BTB solution at 30 °C, 10 mA/cm^2, and pH 4.7.

20 mg/L		40 mg/L		60 mg/L		80 mg/L		100 mg/L	
Time (min)	Abs.	Time (min)	Abs.	Time (min)	Abs.	Time (min)	Abs.	Time (min)	Abs.
0	0.138	0	0.232	0	0.269	0	0.518	0	0.707
5	0.081	5	0.15	5	0.188	5	0.389	5	0.567
10	0.047	10	0.01	10	0.13	10	0.291	10	0.455
15	0.032	15	0.066	15	0.094	15	0.212	15	0.341
20	0.021	20	0.049	20	0.07	20	0.163	20	0.26
25	0.012	25	0.029	25	0.045	25	0.113	25	0.205
30	0.008	30	0.02	30	0.032	30	0.082	30	0.149
35	0.005	35	0.016	35	0.024	35	0.06	35	0.12
40	0.004	40	0.011	40	0.021	40	0.053	40	0.1
45	0.004	45	0.01	45	0.019	45	0.044	45	0.085
50	0.003	50	0.009	50	0.017	50	0.042	50	0.075
55	0.003	55	0.008	55	0.016	55	0.035	55	0.064
60	0.002	60	0.005	60	0.01	60	0.028	60	0.054

Table S2. Electrocoagulation results for treatment of BTB solution at 30 °C, 20 mA/cm^2, and pH 4.7.

20 mg/L		40 mg/L		60 mg/L		80 mg/L		100 mg/L	
Time (min)	Abs.	Time (min)	Abs.	Time (min)	Abs.	Time (min)	Abs.	Time (min)	Abs.
0	0.138	0	0.232	0	0.269	0	0.518	0	0.707
5	0.073	5	0.139	5	0.181	5	0.368	5	0.55
10	0.041	10	0.081	10	0.107	10	0.24	10	0.385
15	0.027	15	0.06	15	0.083	15	0.197	15	0.309
20	0.018	20	0.047	20	0.069	20	0.161	20	0.261
25	0.011	25	0.039	25	0.055	25	0.133	25	0.216
30	0.008	30	0.033	30	0.048	30	0.111	30	0.189
35	0.005	35	0.027	35	0.04	35	0.093	35	0.159
40	0.003	40	0.023	40	0.034	40	0.075	40	0.139
45	0.002	45	0.017	45	0.028	45	0.062	45	0.113
50	0.002	50	0.012	50	0.02	50	0.048	50	0.081
55	0.001	55	0.008	55	0.013	55	0.032	55	0.063
60	0.001	60	0.003	60	0.005	60	0.022	60	0.036

Table S3. Electrocoagulation results for treatment of BTB solution at 50 °C, 20 mA/cm^2, and pH 4.7.

20 mg/L		40 mg/L		60 mg/L		80 mg/L		100 mg/L	
Time (min)	Abs.	Time (min)	Abs.	Time (min)	Abs.	Time (min)	Abs.	Time (min)	Abs.
0	0.138	0	0.232	0	0.269	0	0.518	0	0.707
5	0.054	5	0.111	5	0.141	5	0.321	5	0.509
10	0.02	10	0.048	10	0.083	10	0.2	10	0.31
15	0.008	15	0.022	15	0.04	15	0.093	15	0.176
20	0.002	20	0.009	20	0.017	20	0.054	20	0.103
25	0.001	25	0.005	25	0.013	25	0.039	25	0.08
30	0.001	30	0.004	30	0.011	30	0.033	30	0.07
35	0.001	35	0.003	35	0.007	35	0.024	35	0.053
40	0.001	40	0.003	40	0.005	40	0.017	40	0.045
45	0.001	45	0.002	45	0.004	45	0.014	45	0.04
50	0.001	50	0.002	50	0.003	50	0.01	50	0.034
55	0.001	55	0.001	55	0.002	55	0.007	55	0.028
60	0.001	60	0.001	60	0.001	60	0.005	60	0.015

Table S4. Effect of initial dye concentration and time on BTB solution treatment using electrocoagulation at 10 mA/cm^2, pH 4.7, and 30 °C.

20 mg/L		40 mg/L		60 mg/L		80 mg/L		100 mg/L	
Time (min)	Removal efficiency	Time (min)	Removal efficiency	Time (min)	Removal efficiency	Time (min)	Removal efficiency	Time (min)	Removal efficiency
0	0	0	0	0	0	0	0	0	0
5	41	5	35.4	5	30.1	5	24.9	5	19.8
10	66.2	10	58.4	10	51.7	10	43.9	10	35.7
15	76.9	15	71.6	15	65.1	15	59.1	15	51.7
20	84.7	20	79	20	74.1	20	68.5	20	63.2
25	91.4	25	87.6	25	83.2	25	78.1	25	71
30	94.3	30	91.5	30	88.2	30	84.1	30	78.9
35	96.5	35	93.2	35	91.1	35	88.5	35	83
40	97	40	95.1	40	92.3	40	89.7	40	86.3
45	97.3	45	95.7	45	93	45	91.6	45	88
50	97.5	50	96	50	93.5	50	91.9	50	89.4
55	97.8	55	96.6	55	94.2	55	93.2	55	91
60	98.6	60	97.7	60	96.1	60	94.6	60	92.3

Table S5. Effect of initial dye concentration and time on BTB solution treatment using electrocoagulation at 20 mA/cm^2, pH 4.7, and 30 °C.

20 mg/L		40 mg/L		60 mg/L		80 mg/L		100 mg/L	
Time (min)	Removal efficiency	Time (min)	Removal efficiency	Time (min)	Removal efficiency	Time (min)	Removal efficiency	Time (min)	Removal efficiency
0	0	0	0	0	0	0	0	0	0
5	47.3	5	40.2	5	32.6	5	28.9	5	22.2
10	70.2	10	65	10	60.1	10	53.7	10	45.5
15	80.3	15	74.2	15	68.9	15	62	15	56.3
20	86.6	20	79.7	20	74.3	20	68.9	20	63.1
25	91.7	25	83.4	25	79.5	25	74.3	25	69.4
30	94.2	30	85.9	30	82	30	78.5	30	73.3
35	96.3	35	88.2	35	85.1	35	82.1	35	77.5
40	97.5	40	90.1	40	87.4	40	85.5	40	80.3
45	98.2	45	92.5	45	89.6	45	88.1	45	84
50	98.9	50	95	50	92.5	50	90.8	50	88.6
55	99.3	55	96.7	55	95.1	55	93.9	55	91.1
60	99.9	60	98.9	60	98.2	60	95.7	60	94.9

Table S6. Effect of initial dye concentration and time on BTB solution treatment using electrocoagulation at 20 mA/cm^2, pH 4.7, and 50 °C.

20 mg/L		40 mg/L		60 mg/L		80 mg/L		100 mg/L	
Time (min)	Removal efficiency	Time (min)	Removal efficiency	Time (min)	Removal efficiency	Time (min)	Removal efficiency	Time (min)	Removal efficiency
0	0	0	0	0	0	0	0	0	0
5	60.8	5	52.3	5	47.5	5	38.1	5	28
10	85.8	10	79.1	10	69.3	10	61.4	10	56.1
15	94.5	15	90.5	15	85.5	15	82	15	75.1
20	98.8	20	96.1	20	93.5	20	89.5	20	85.4
25	99	25	97.8	25	95.1	25	92.5	25	88.7
30	99.4	30	98.1	30	95.9	30	93.7	30	90.1
35	99.4	35	98.7	35	97.5	35	95.4	35	92.5
40	99.5	40	98.9	40	98	40	96.7	40	93.7
45	99.6	45	99.2	45	98.5	45	97.3	45	94.5
50	99.6	50	99.3	50	99.1	50	98.1	50	95.2
55	99.8	55	99.4	55	99.2	55	98.6	55	96.1
60	99.8	60	99.7	60	99.4	60	99.1	60	97.9

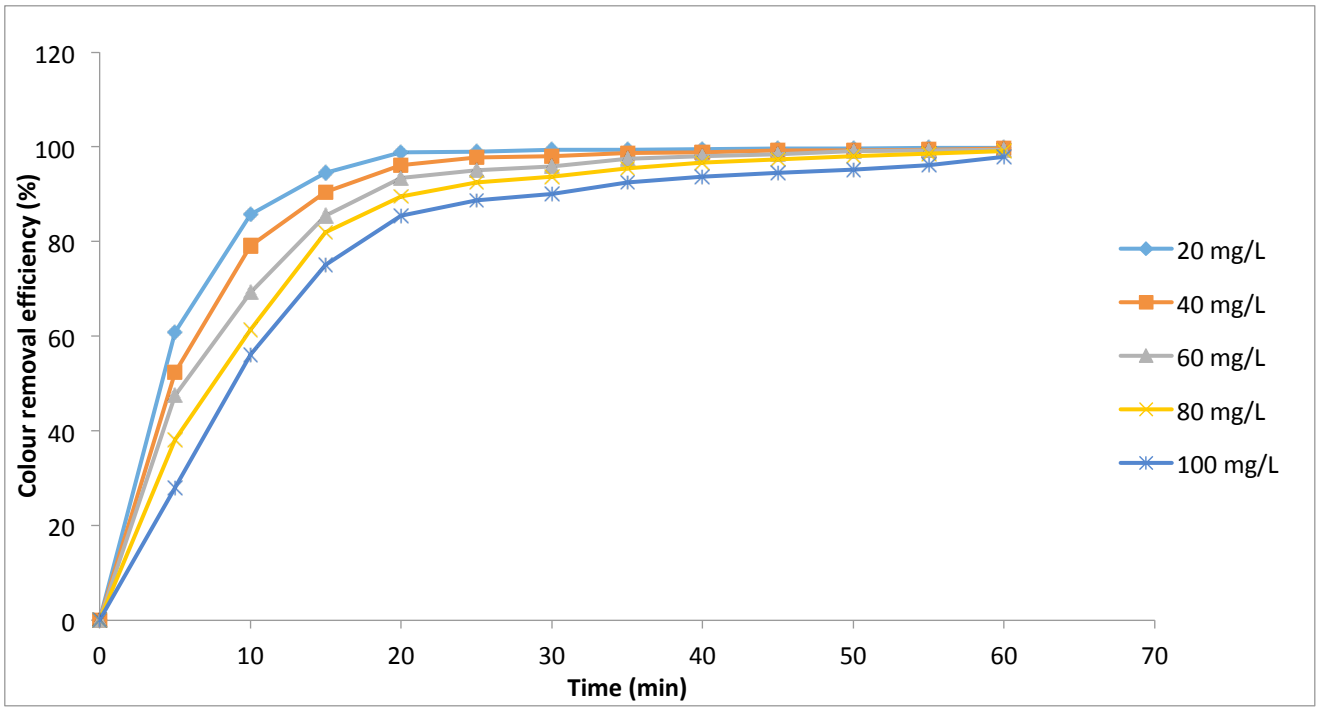

Figure S1. A plot of color removal efficiency versus time during EC process of BTB solution at 20 mA/cm^2, 50 °C, and pH 4.7.

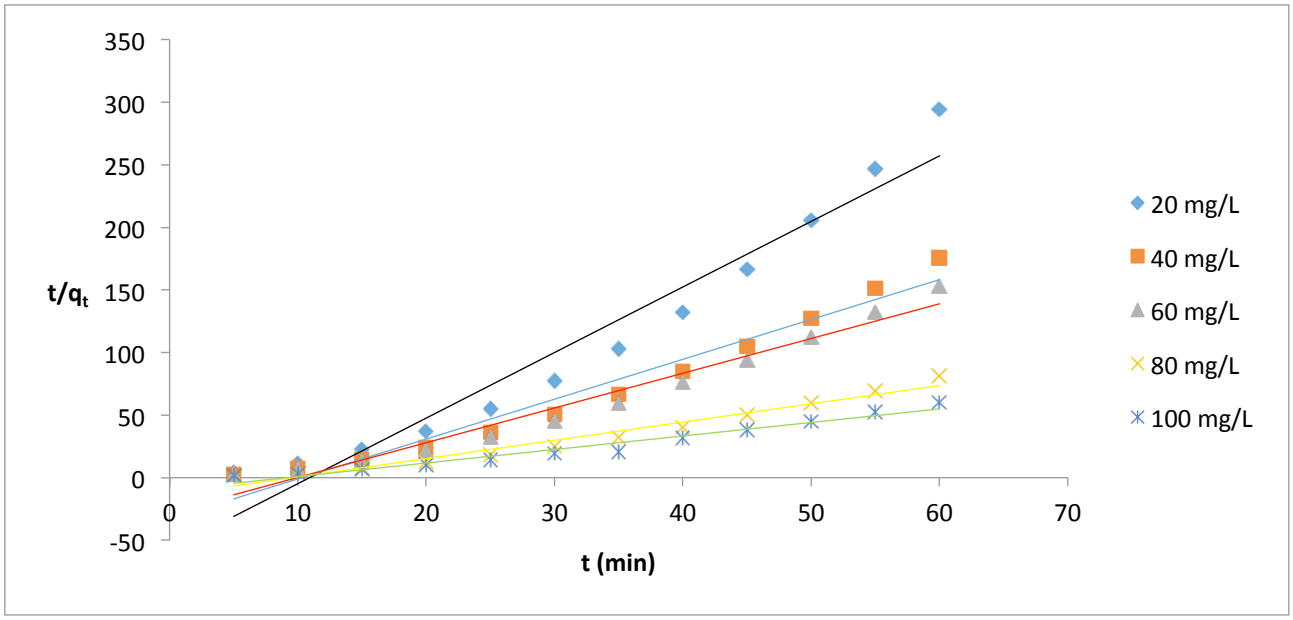

Figure S2. Pseudo-second-order plot of electrocoagulation of BTB solution at 20 mA/cm^2, pH 4.7, and 30 °C.

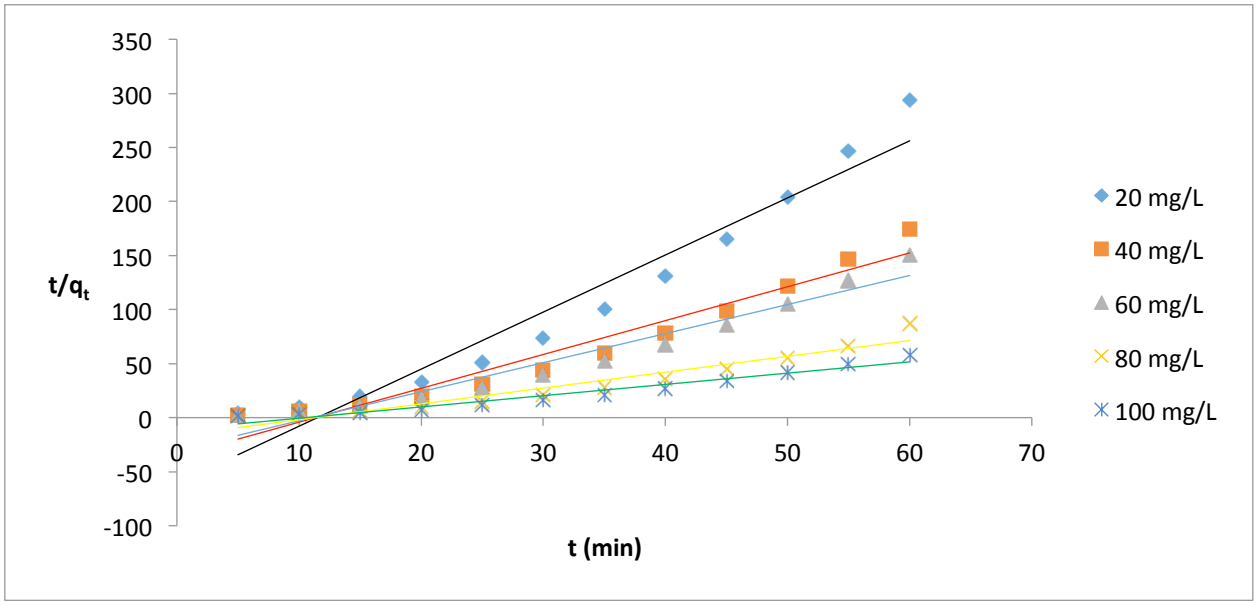

Figure S3. Pseudo-second-order plot of electrocoagulation of BTB solution at 20 mA/cm^2, pH 4.7, and 50 °C.

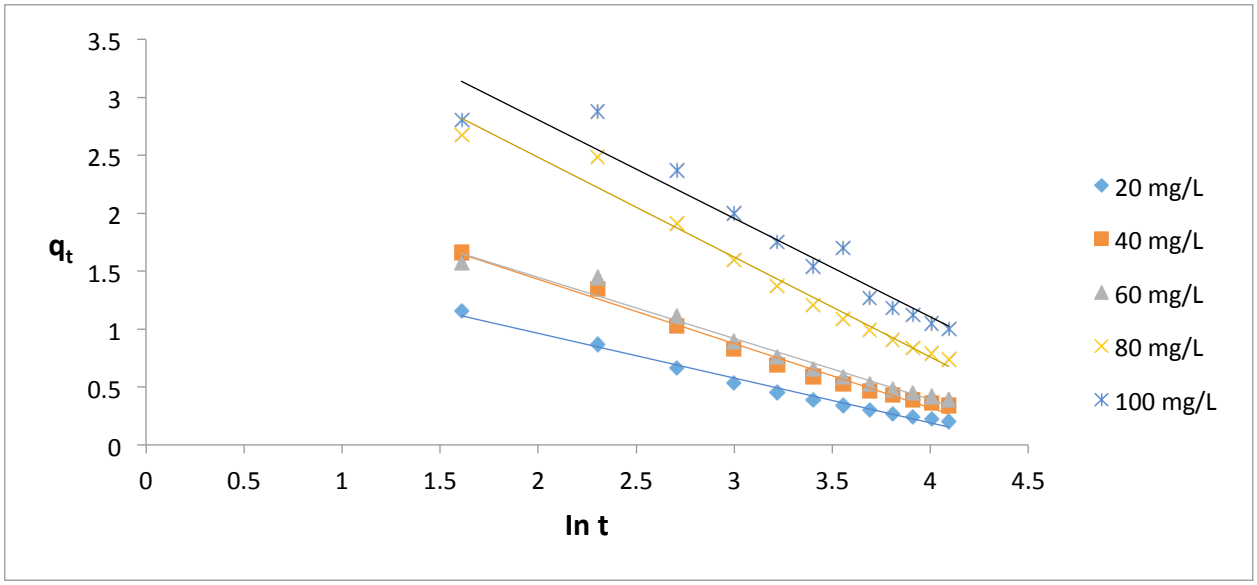

Figure S4. Elovich kinetic model plot of the electrocoagulation of BTB solution at 20 mA/cm^2, pH 4.7, and 30 °C.

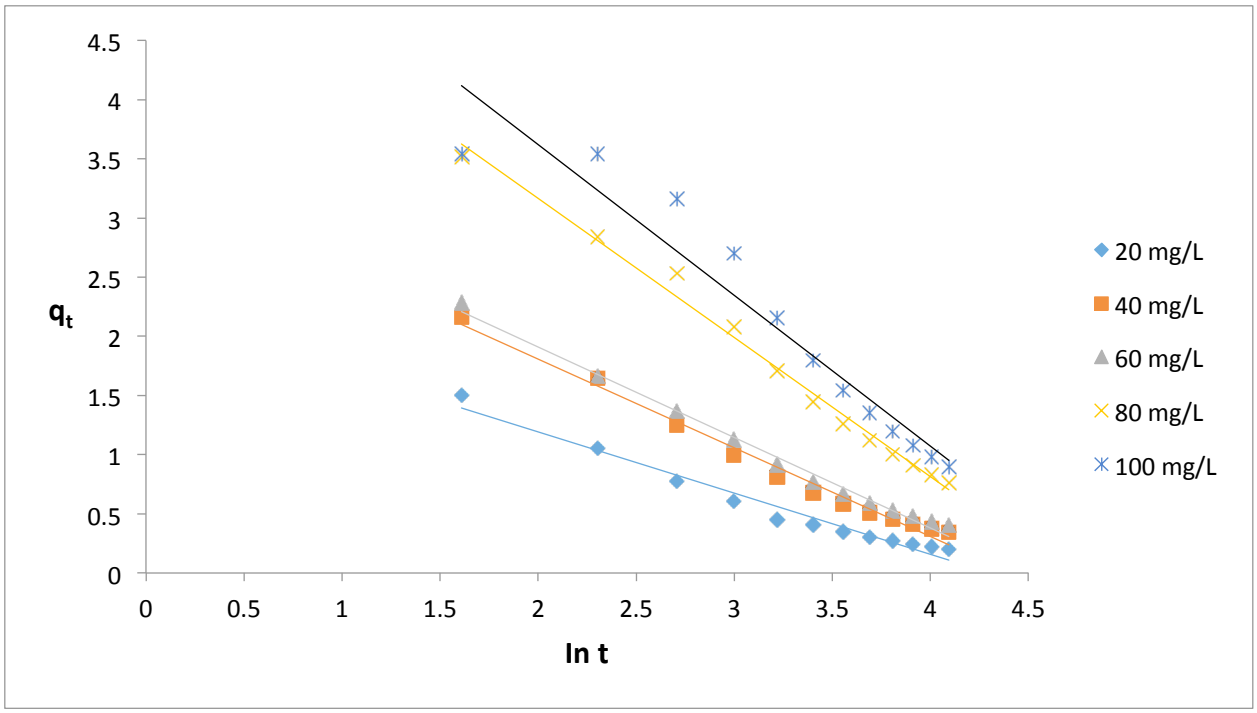

Figure S5. Elovich kinetic model plot of the electrocoagulation of BTB solution at 20 mA/cm^2, pH 4.7, and 50 °C.

Table S7. Pseudo-second-order kinetic parameters for the electrocoagulation of BTB solution.

		Pseudo-second-order						
	30 °C				50 °C			
Conc.	k_2	q_e	q_{ecalc}	R^2	k_2	q_e	q_{ecalc}	R^2
(mg/L)	(g mg^{-1} min^{-1})	(mg g^{-1})	(mg g^{-1})		(g mg^{-1} min^{-1})	(mg g^{-1})	(mg g^{-1})	
20	–0.48	0.191	0.34	0.95	–0.461	0.189	0.609	0.946
40	–0.309	0.314	0.524	0.962	–0.277	0.319	0.998	0.946
60	–0.279	0.361	0.585	0.966	–0.242	0.372	1.128	0.948
80	–0.153	0.686	1.086	0.968	–0.129	0.683	2.076	0.929
100	–0.118	0.926	1.4	0.963	–0.099	0.959	2.702	0.951

Table S8. Elovich kinetic parameters for the electrocoagulation of BTB solution.

		Elovich model				
		30 °C			50 °C	
Conc.	α	β	R^2	α	β	R^2
(mg/L)	(mg g^{-1})	(g mg^{-1})		(mg g^{-1})	(g mg^{-1})	
20	–0.0043	–2.591	0.986	–0.007	–1.934	0.969
40	–0.0057	–1.801	0.985	–0.0091	–1.335	0.986
60	–0.0046	–1.898	0.975	–0.0085	–1.309	0.991
80	–0.0065	–1.161	0.977	–0.0108	–0.851	0.991
100	–0.0042	–1.176	0.933	–0.01	–0.786	0.925

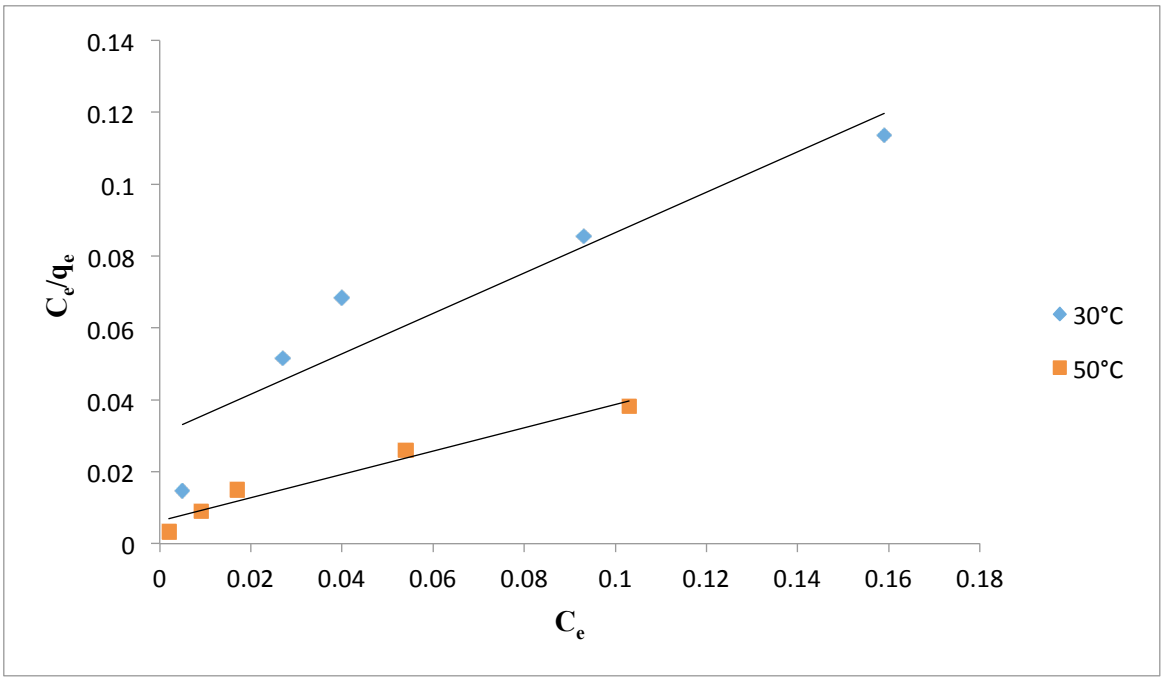

Figure S6. Langmuir adsorption isotherm plot for the electrocoagulation of BTB solution.

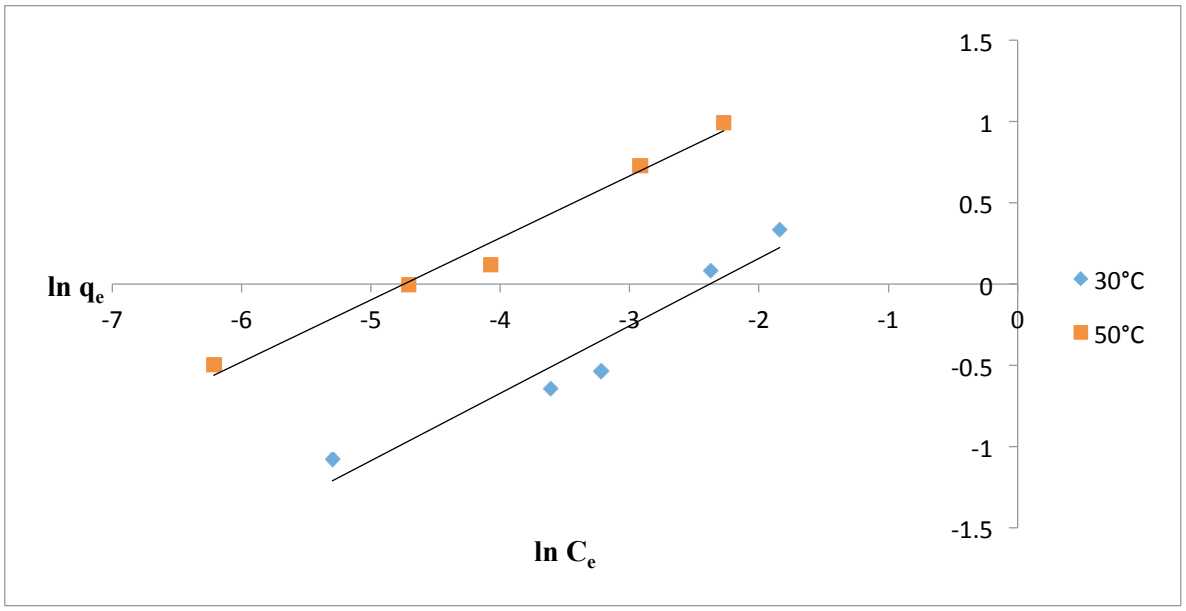

Figure S7. Freundlich adsorption isotherm plot for the electrocoagulation of BTB solution.